

N O T I C E

THIS DOCUMENT HAS BEEN REPRODUCED FROM
MICROFICHE. ALTHOUGH IT IS RECOGNIZED THAT
CERTAIN PORTIONS ARE ILLEGIBLE, IT IS BEING RELEASED
IN THE INTEREST OF MAKING AVAILABLE AS MUCH
INFORMATION AS POSSIBLE

"Made available under NASA sponsorship
in the interest of early and wide dis-
semination of Earth Resources Survey
Program information and without liability
for any use made thereof."

8.0-10.036
CR-162447

USE OF THERMAL INFRARED AND COLOUR INFRARED
IMAGERY TO DETECT CROP MOISTURE STRESS

INTERIM REPORT

March, 1979

R.C. McKenzie¹, N.F. Clark², and J. Cihlar³

Sponsored By:

ALBERTA REMOTE SENSING CENTER
CANADA CENTRE FOR REMOTE SENSING
ALBERTA AGRICULTURE

(E80-10036) USE OF THERMAL INFRARED AND
COLOUR INFRARED IMAGERY TO DETECT CROP
MOISTURE STRESS Interim Report (Canada
Centre for Remote Sensing, Ottawa) 36 p
HC A03/MF A01

N80-15530

Unclas
00036

CSSL 02C G3/43

- 1 Soil and Water Specialist, Alberta Agriculture,
Irrigation Division, Brooks.
- 2 Irrigation Technologist, Alberta Agriculture,
Irrigation Division, Brooks.
- 3 Environmental Scientist, Canada Centre for Remote
Sensing, Ottawa.

RECEIVED

NOV 30 1979

SIS/902.6

HCM 054 TYPE II

TABLE OF CONTENTS

	<u>Page</u>
1. INTRODUCTION	1
2. DATA ACQUISITION	1
3. DATA ANALYSIS	2
4. RESULTS AND DISCUSSION	3
5. FUTURE WORK	5
6. REFERENCES	6
FIGURE 1	7
FIGURE 2	8
FIGURE 3	9
FIGURE 4	10
TABLE 1	11
TABLE 2	12
TABLE 3	11
APPENDIX	13

LIST OF FIGURES

- FIGURE 1. Within-plot apparent temperature ranks plotted against the root zone water content. Ranks 1 through 12 were assigned to each treatment/replicate combination within a crop and time of flight.
- FIGURE 2. Daytime and nighttime apparent temperature as a function of available water in the root zone for irrigation plots.
- FIGURE 3. Daytime apparent temperature as a function of available water in the root zone for irrigated and non irrigated fields with various crops.
- FIGURE 4. Daytime apparent temperature as a function of the density difference between IR-sensitive and red-sensitive layers of the colour infrared transparencies.
- APPENDIX A night infrared thermal analogue image (as seen under a density slicer) of a faba bean irrigation plot and surrounding area.

LIST OF TABLES

TABLE 1. Correlation matrix for data set DS1 (all data, 18 points).

TABLE 2. Correlation coefficients between available soil water and remote sensing variables for three data sets.

TABLE 3. Correlation matrix for data set DS3 (irrigated fields only, DS3).

1. INTRODUCTION

In southern Alberta, intensive agriculture is possible only on irrigated land. Irrigated crops must be provided with adequate amounts of water, but the periodic water shortages (such as in 1977 due to less-than-normal rainfall) and the expanding total area of irrigated land demand that water use be made more efficient. Thus, the 1978 Oldman River Report recommended that irrigation scheduling programs be enlarged and improved to increase water use efficiency. However, previous irrigation scheduling services have encountered difficulties because of the inability to adequately monitor moisture status of crops. Since crop water requirements may differ from one field to another as well as within fields, a complete soil moisture sampling program would be very expensive.

Preliminary studies conducted in the U.S. (e.g. Millard et al., 1977) have shown that crop moisture stress may be detected by using aircraft remote sensing data. The purpose of the project described here was to evaluate whether remote sensing data can provide information that would be useful to supplement ground observation in an irrigation scheduling program.

2. DATA ACQUISITION

Fifteen farm fields with different crops (irrigated corn, alfalfa, fall rye, potatoes, flax, and peas; unirrigated wheat, summerfallow, and native range) were chosen for the study. Five small experimental plots, each containing three water treatments and four replicates, were also included. They contained potatoes and carrots (at Cassils), cabbage and mustard (Duchess), and faba beans (Rockyford).

Two missions were undertaken by Canada Centre for Remote Sensing (CCRS) on June 21 and August 5, 1978. Each mission consisted of a day flight during which colour infrared and thermal infrared imagery were simultaneously obtained, and a night flight with only thermal imagery being collected. CCRS acquired photographs at 1:4,100 for the irrigation plots and 1:50,000 for all sites.

Two additional flights were made on July 24 and August 18 by Kenting Air Services on a contract from the Alberta Remote Sensing Centre. They obtained day colour infrared photographs on a 1:2,500 scale from the irrigation plots and 1:10,000 scale for all sites.

At the time of each flight, the irrigation plots were sampled to determine soil moisture gravimetrically. Twelve sites on each irrigation plot were sampled, one for each of the 3 water treatments and four replicates. Samples from

Four depths (30cm increments) were taken at each sample site. At the time of each CCRS flight, twelve to fifteen fields were sampled, while seven fields were sampled at the time of each Kenting flight. Six sites were sampled in each farm field and four depths (30cm increments) were taken per sample site. The above sampling procedure thus produced approximately 1,800 soil moisture samples during the experiment.

Soil texture was determined for each site, and both field capacity (FC) and permanent wilting point (PWP) were derived from the soil texture and available data (both published and unpublished). Using the above parameters and root depths obtained from the Alberta Agriculture irrigation scheduling program, the amount of available water (AW, in percent) was determined for each irrigation plot and each of the six sites within the farm fields as follows:

$$AW = \frac{WC - PWP}{FC - PWP} \times 100, \quad (\%)$$

where WC is the total water content in cm and all three variables refer to the root zone.

In addition to soil moisture samples, ground colour infrared photographs and normal colour photographs of the irrigation plots and farm fields were taken at the time of each flight. Measurements of crop canopy temperatures were also made with a portable radiation thermometer PRT-5 a number of times during the summer.

3. DATA ANALYSIS

Colour infrared aerial photographs processed as positive transparencies and thermal images in both analogue and level-sliced form were used for the analysis. Densitometric measurements of each sampled field site (on the small scale photography) and irrigation plot (large scale photography) were made using a Macbeth transmission densitometer TD-504, separately for each emulsion layer.

Thermogram analysis was carried out in three steps. First, analogue low altitude thermograms were displayed on a density slicer and the individual treatment/replicate combinations were ranked from coldest (=1) to warmest (=12), separately for day and night data. An average rank value was then computed for each treatment/plot (crop) /time (day or night) combination. Secondly, the apparent temperature "slice" was determined for each sampled site on the low altitude (irrigated plots) and high altitude (farm fields) level-sliced

thermograms. This procedure was considered necessary because the level sliced thermograms contained relatively coarse temperature slices, particularly for the daytime images. As the third step, regression analysis was carried out using the farm fields data. For this analysis, average values were computed for all sites within one field which were located in the same temperature "slice"; emulsion densities and AW values were included in this averaging process. Results presented in the following section refer to data obtained on August 5, 1978. These data were given higher priority because moisture stress was more evident at that time.

4. RESULTS AND DISCUSSION

Figure 1 shows the plot of apparent temperature rank as a function of available water. Each point is an average of four rank values (4 replicates/treatment). The apparent temperature increased with decreasing available water in the range of 110 to 40%. The relative response to changing moisture availability was similar for all crops studied and for both day and night measurements, although its uniformity was lower for cabbage and mustard (Duchess site) than for other crops. It should be stressed, however, that neither absolute temperature values nor the slope (sensitivity) can be derived from Figure 1.

Apparent temperature ranges of the five irrigation plots are shown in Figure 2 for both day and night data. Night temperature values were lower and had a low or no sensitivity to available water deficiency than the daytime measurements. The absolute temperature ranges also differed between crops for similar available water (AW) amounts, even for adjacent crops at the Duchess and Cassils sites. Due to the coarseness of the daytime temperature "slices", no final conclusions concerning the magnitude of differences caused by crop cover and time of day can be drawn from the data. It is encouraging, however, that the daytime temperature decreased consistently with increasing AW content for all plots. It is also of interest to note that the irrigation plots apparent temperature levels were higher than those for large fields at comparable soil moisture conditions. This might be due to advection effects but the available data do not allow establishing the reason with certainty.

Only daytime temperature ranges of the farm fields were available for this interim report. In Figure 3, these values were plotted against corresponding available water contents for all fields. The data included irrigated and dry-land crops, rangeland, and a fallow field. The apparent temperatures exhibited a general decrease with increasing water content, but a considerable scatter is

evident as well. Energy balance considerations (Cihlar, 1976) as well as previous studies indicate that surface cover - particularly the relative proportions of green crop cover and bare ground - affects the surface temperature measured by an infrared remote sensor. Previous remote sensing studies established that the ratio of radiation reflected in near infrared and red portions of the electromagnetic spectrum increases with increasing crop cover. Therefore, we attempted to quantify the amounts of plant cover by using DRG which is defined as the difference between CIR transparency densities of the infrared - sensitive and the red - sensitive emulsion layers. A plot of DRG vs. apparent temperature (Figure 4) showed a close direct linear relationship between the two variables. Furthermore, the points were grouped into two clusters which coincided with irrigated (negative DRG) and dryland (positive DRG) sites. When the dryland sites were identified in Figure 3, they were found to be the highest apparent temperature values encountered. In other words, the lack of ground cover caused apparent temperature increase due to the increased exposure of bare soil. If only irrigated sites are considered in Figure 3, the relationship between temperature and available water is more closely defined. The goodness of fit of the temperature-water content relationship for irrigated fields (Figure 3) depends on the positions of three "outlier" data points (at AW = -11, 17 and 91%) which must be determined from more precise temperature data.

Relationships between remote sensing and ground variable were quantified using correlation analysis. Mid-values of the temperature "slices" were used in lieu of apparent temperatures. The following variables were included for all farm fields (a total of 18 data points):

- DR = Density of the near IR - sensitive layer, dimensionless;
- DG = Density of the red - sensitive layer, dimensionless;
- DRG = Difference between DR and DG, dimensionless;
- T_{ap} = Apparent temperature (day value), °C;
- AW = Available water in the root zone, %.

The resulting correlation matrix (Table 1) shows that the apparent temperature was closely related to the difference DRG between red and green emulsion densities, which is in turn affected by the amount of green cover above the soil surface. The correlation between available water and T_{ap} was quite low (-0.41). Correlation coefficients between T_{ap} (dependent variable) and several independent variables were high when DRG was used, and fairly low otherwise (Table 2, data set DS1). The accuracy of predicting available water from T_{ap} did not improve significantly when DRG was also used, and increased partially

after DR was added to the independent variables ($r = 0.47$, Table 2). The low improvement of the correlation coefficient suggests that DRG was only weakly related to the available water, and therefore did not improve the AW prediction. Since a definite relationship between soil water available at a given time and surface cover cannot be expected, variable surface cover would appear to be an intrinsic limitation of plant moisture stress determination through thermal infrared remote sensing.

Due to various crop types and degrees of surface cover being present in the data set and since the T_{ap} values used were only approximate, an attempt was made to remove some of the uncertainties by reducing the data set in two ways. First, three seemingly anomalous points (at AW = -11, 17 and 91%) were omitted to form a data set DS2 with 15 points. Secondly, irrigated fields from data set DS2 were put into data set DS3 which therefore contained 9 points. On the CIR transparencies, irrigated fields appeared to have a higher plant cover, were shown in deeper red colours, and soil was visible relatively seldom compared to the dryland fields. Correlation coefficients for various relationships were calculated for DS2 and DS3 in the same manner as for DS1.

The DS2 results were similar to those for DS1. Some improvements occurred, but were not very large even after including DRG and DR values (Table 2). In contrast, considerable improvement of AW prediction was found for DS3 (Table 3). In this case, DRG and T_{ap} together explained 70% of the total variability of the AW values encountered in the irrigated farm fields data ($r = 0.84$, Table 2).

The above results were derived from averages of several soil moisture samples per farm field and a relatively crude measure of the apparent temperature. Although additional data and a more thorough analysis will be required to arrive at definitive conclusions, findings to date are consistent with the following statement. In the presence of variable plant cover (primarily percent cover) and variable available water content, the remotely sensed apparent temperatures correlate closely with plant cover and poorly with soil water. To the extent that plant cover is not systematically related to available soil water, AW values may not be reliably predicted from the thermal infrared data. On the other hand, if plant cover is uniform and the soil surface is shown in a minor way, the thermal data indicate plant stress and consequently available water in the soil profile.

5. FUTURE WORK

To provide definitive analysis and interpretation of the above indicated trends, the following tasks will be carried out:

- (i) Digitize daytime thermal infrared data for the 5 August 1978 flight
- (ii) Extract apparent temperature values for individual sampled sites on both irrigation plots and farm fields.
- (iii) Extract apparent temperatures for the nighttime data from level-sliced thermograms.
- (iv) Calculate day-night temperature differentials for 5 August 1978.
- (v) Analyze the relationships between field data, thermal data, and photographic density measurements.
- (vi) Confirm the validity of the conclusions using data from 20 June 1978 over the same area.

6. REFERENCES

- Cihlar, J. 1976. Soil moisture determination by thermal infrared remote sensing. Proceedings of the Workshop on Remote Sensing of Soil Moisture and Groundwater, 8-10 November 1976, Toronto, Ontario.
- Millard, J.P., R.D. Jackson, R.G. Goettelman, R.J. Reginato, S.B. Idso, and R.L. LaPado. 1977. Airborne monitoring of crop canopy temperatures for irrigation scheduling and yield prediction. Proceedings of the 11th International Symposium on Remote Sensing of Environment, Ann Arbor, MI 1453-1461.

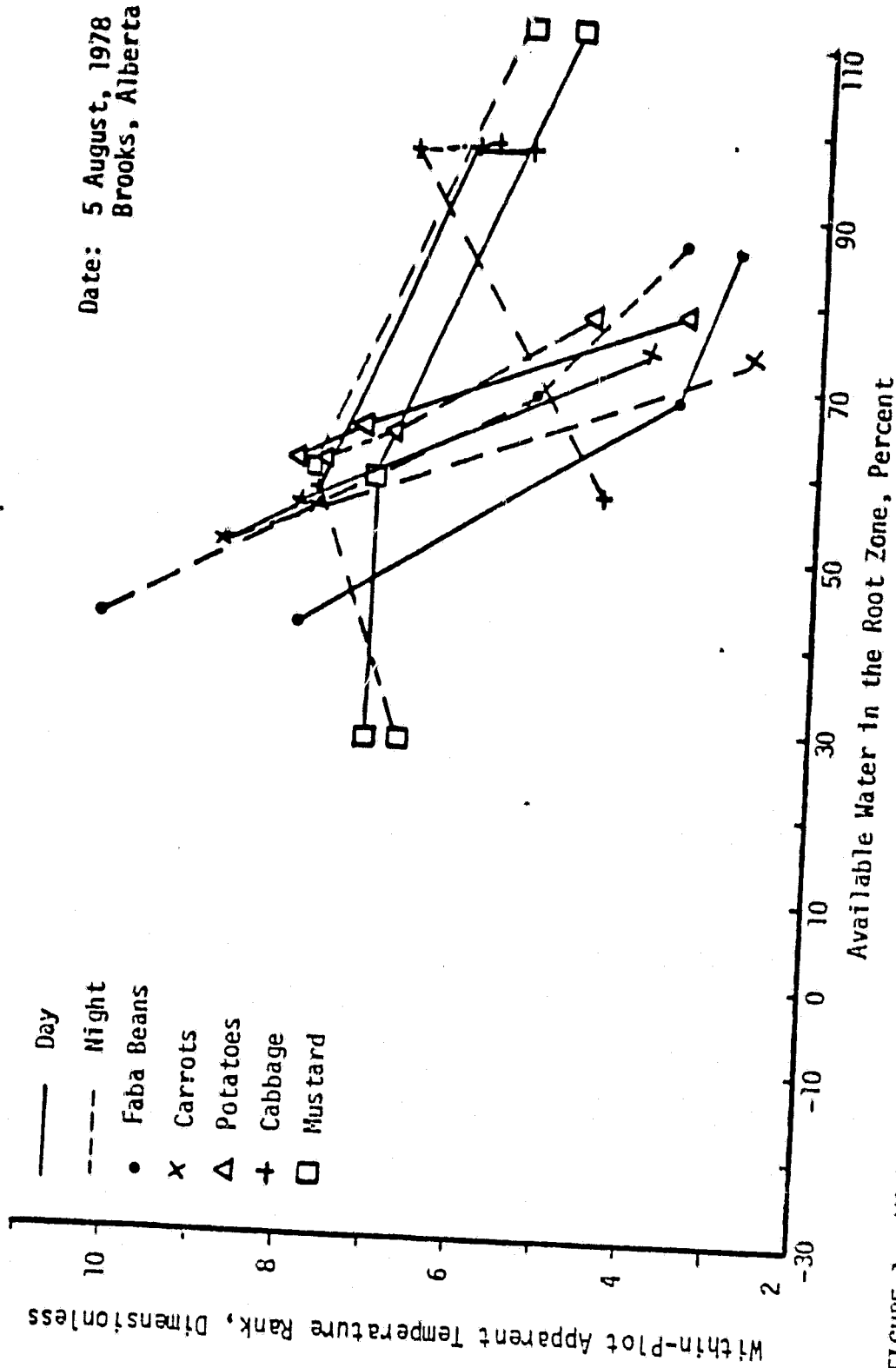


FIGURE 1. Within-Plot apparent temperature ranks plotted against the root zone water content. Ranks 1 through 12 were assigned to each treatment-replicate combination within a crop and time of flight.

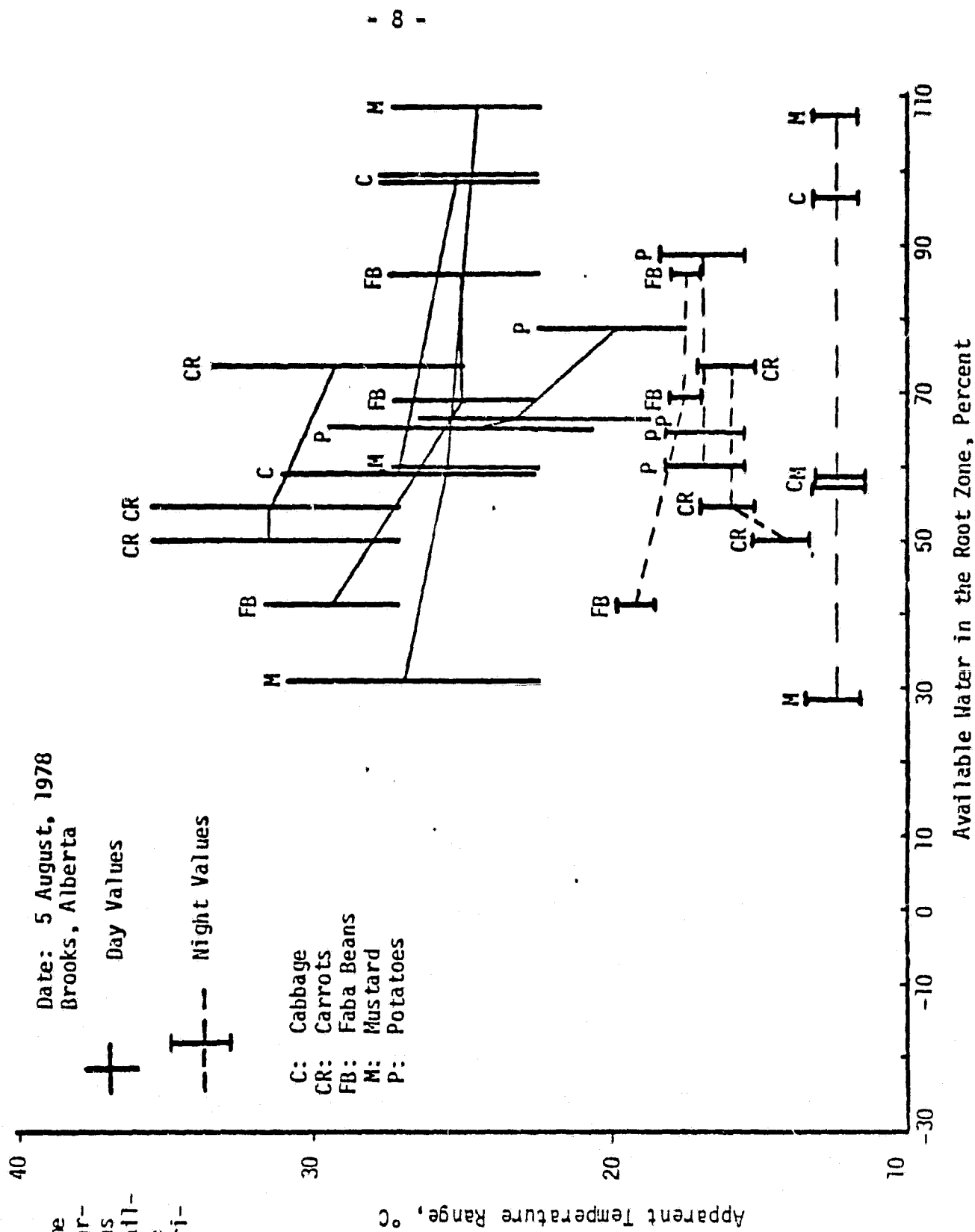
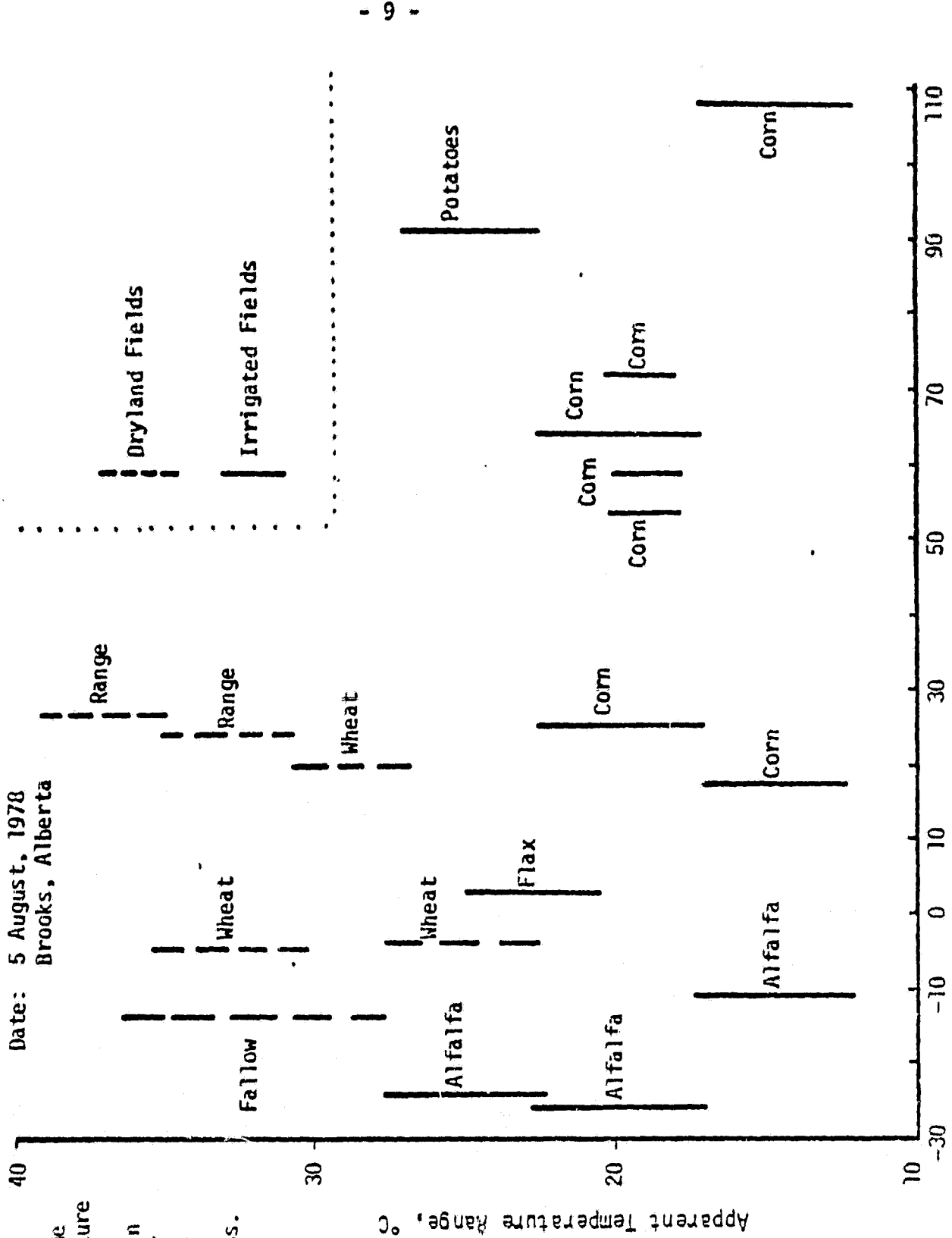


FIGURE 2. Daytime and nighttime apparent temperature as a function of available water in the root zone for irrigation plots

Available Water in the Root Zone, Percent

Apparent Temperature Range, °C



Date: 5 August, 1978
Brooks, Alberta

FIGURE 3. Daytime apparent temperature as a function of available water in the root zone for irrigated and non irrigated fields with various crops.

Apparent Temperature Range, °C

Available Water in the Root Zone, Percent

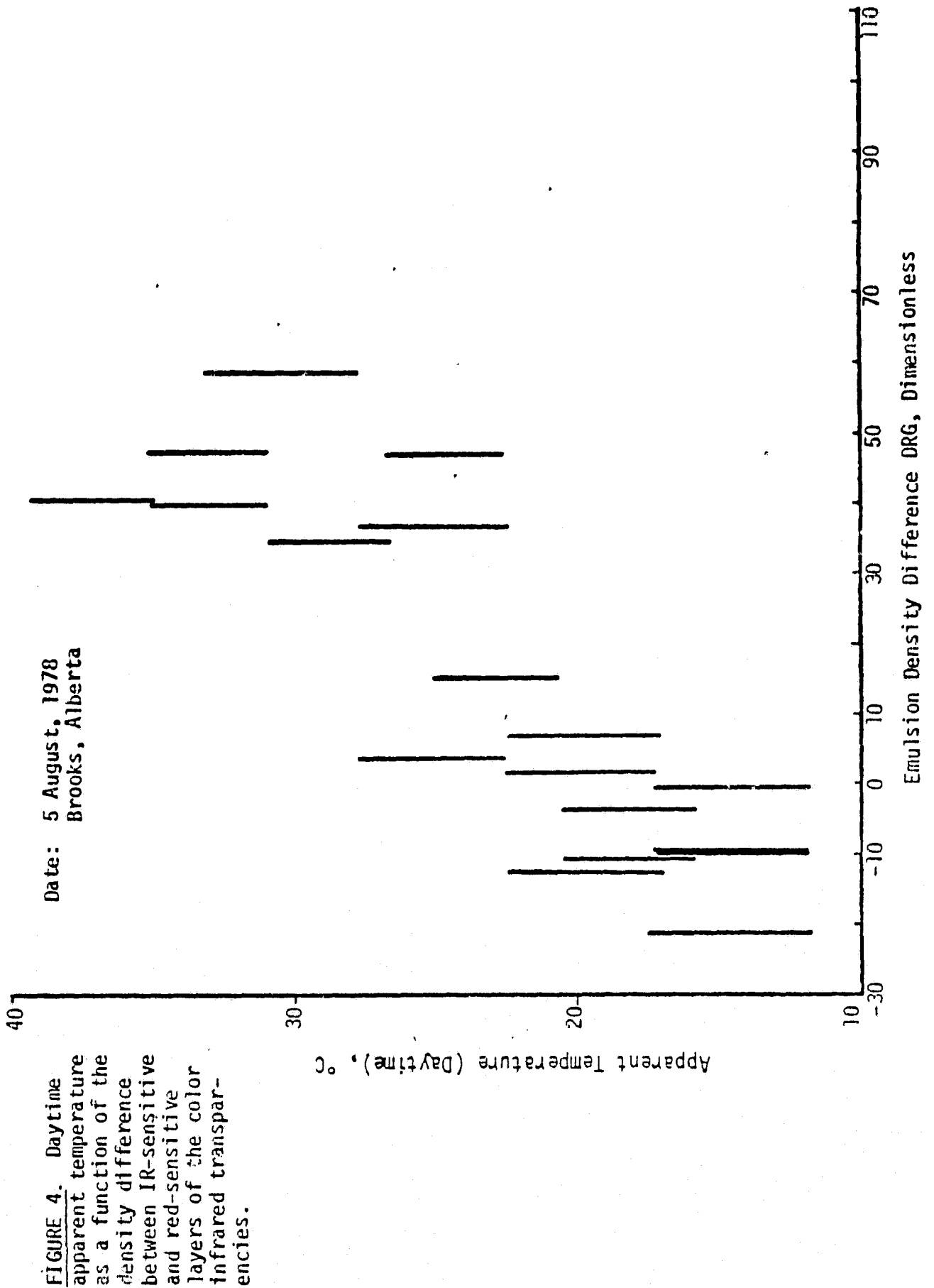


Table 1. Correlation matrix for data set DS1
(all data, 18 points). **

DR	1.00				
DG	0.31	1.00			
DRG	0.43	-0.72	1.00		
T _{ap}	-.27	-0.70	0.86	1.00	
AW	-0.33	-.14	-0.37	-0.41	1.00
	DR	DG	DRG	T _{ap}	AW

** 0.01 significance level: 0.58

Table 3. Correlation matrix for data set DS3
(irrigated fields only, DS3)**

DR	1.00				
DG	0.81	1.00			
DRG	0.08	-0.08	1.00		
T _{ap}	0.22	-0.05	0.52	1.00	
AW	-0.06	-0.01	-0.28	-0.80	1.00
	DR	DG	DRG	T _{ap}	AW

** 0.01 significance level: 0.62

Table 2. Correlation coefficients between available soil water and remote sensing variables for three data sets.

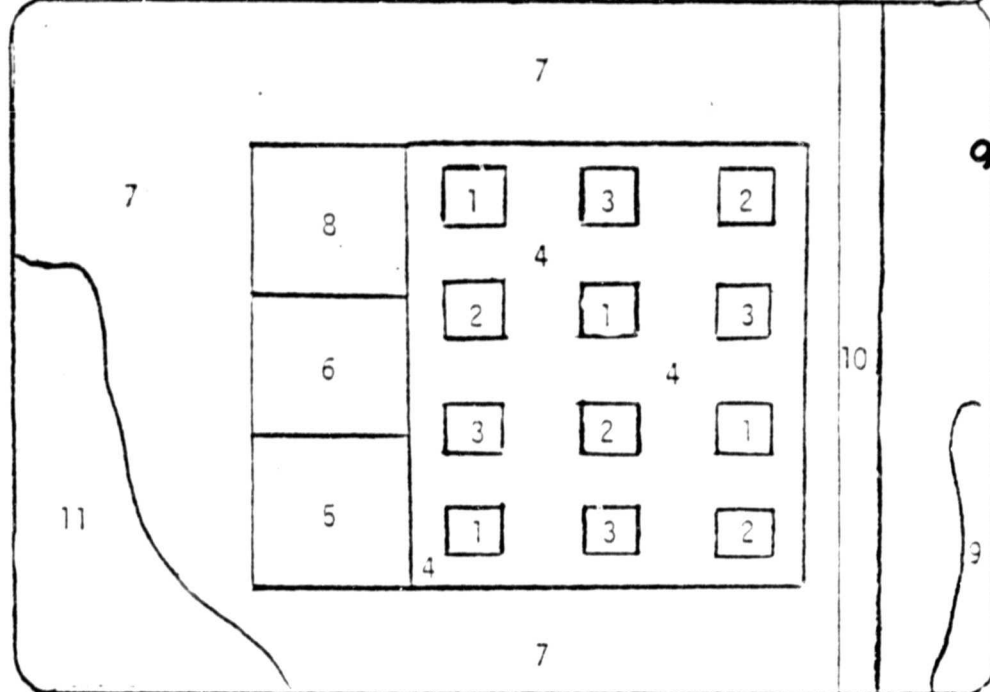
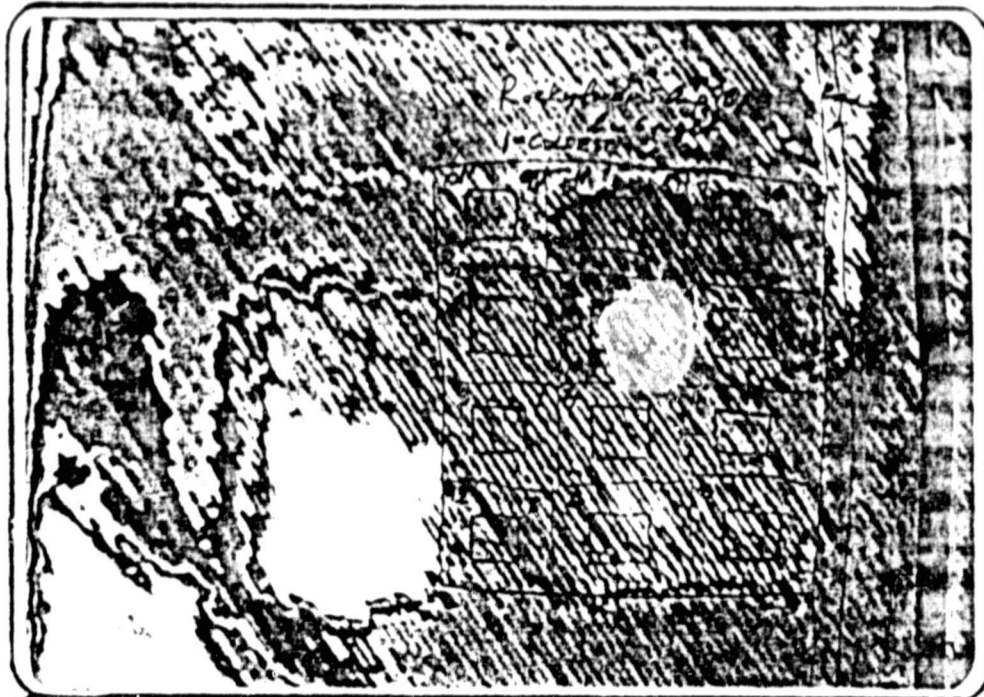
VARIABLES		CORRELATION COEFFICIENT FOR DATA SET †		
DEPENDENT	INDEPENDENT	DS1	DS2	DS3
T _{ap}	AW	0.41	0.54	0.80
T _{ap}	DRG	0.86	0.82	0.40
T _{ap}	AW, DRG	0.86	0.89	0.87
T _{ap}	AW, DRG, DR	0.88	0.89	0.88
AW	T _{ap} , DRG	0.41	0.55	0.84
AW	T _{ap} , DRG, DR	0.47	0.57	0.85
		N = 18	N = 15	N = 9

† Data set DS1: All data (18 points)

† Data set DS2: Outlier points excluded (15 points)

† Data set DS3: Only irrigated fields of data set 2 (9 points)

A Night Infrared Thermal Analogue Image (As Seen Under A Density Slicer) of A Faba Bean Irrigation Plot and Surrounding Area



ORIGINAL PAGE IS OF POOR QUALITY

- 1. Water 1 faba bean treatment under moisture stress. 2. Water 2 under slight moisture stress. 3. Water 3 under no moisture stress. 4. Border area of faba bean plots.
- 5. Plots of beans - soybeans, mung beans, faba beans, lentils which were recently irrigated to excess at the same rate as #6 which had a higher water use. 6. Plot of corn, forage sorghum, sorghum-sudangrass, and sorghum which was recently irrigated.
- 7. Wheat not irrigated severe stress. 8. Wild oats and weeds severe stress. 9. Summerfallow. 10. Roadway. 11. Grassland next to irrigation ditch moderate to no stress.

White, yellow, blue, green, red, mauve.
 Coolest → hottest.

REPRODUCIBILITY OF THE ORIGINAL PAGE IS POOR

SOIL WATER CONTENT ESTIMATION IN FALLOW FIELDS FROM AIRBORNE THERMAL SCANNER MEASUREMENTS

by J. Cihlar

*Applications Division,
Canada Centre for Remote Sensing, Ottawa*

T. Sommerfeldt

Agriculture Canada, Research Station, Lethbridge

and B. Paterson

Alberta Agriculture, Irrigation Division, Lethbridge

SUMMARY

The purpose of this study was to determine if the relationship between diurnal surface temperature variations and near-surface soil water content may be used to determine soil water content from airborne measurements. Four flight missions with thermal infra-red and photographic sensors were conducted over an agricultural area in Southern Alberta during clear sky diurnal periods. Soil water content samples expressed in percent of field capacity (PFC), digitized thermal infra-red measurements, apparent temperatures at samples sites, and day minus night temperature differentials ΔT , were obtained. Results confirmed the existence of an inverse linear ΔT , vs PFC relationship under the experimental conditions, with near-surface water content generally the most important ground variable determining ΔT . The ΔT , vs PFC relationship was not improved by considering diurnal air temperature fluctuations, but did show various degrees of improvement when apparent radiances from the visible spectrum were included.

INTRODUCTION

Soil moisture is a very important parameter in studying, monitoring and modifying the behaviour of various land ecosystems (Idso et al, 1975a). The methods developed for its measurement can be divided into two groups (Cihlar and Ulaby, 1975): contact or direct methods which provide moisture estimates for a soil segment specifically examined or measured; and non-contact (or indirect) methods which do not require in situ measurements. The contact methods are costly when implemented over large areas, compared to non-contact methods (water balance and remote sensing approaches) which are less expensive and are therefore of primary interest for large-scale, operational soil moisture monitoring. The potential advantage of remote sensing approach is that every ground element is covered so that there is no need for interpolations or assumptions about the spatial variation of meteorological and ground characteristics.

Three remote sensing techniques appear potentially suitable for satellite applications: thermal infra-red, active microwave, and passive microwave (Cihlar and Ulaby, 1975). The principles involved in the thermal infra-red method have been described by Idso et al (1975b), Idso and Ehler (1976), Reginato et al (1976), Schmugge et al (1978) and Cihlar (1976). For bare soils, it was determined that the difference between maximum and minimum surface temperature during clear-day diurnal periods, ΔT , was inversely related to the soil water content in the top 2 to 4 cm of the soil. The relationship varied with soil texture, but when soil water content was expressed in matrix tension, soil texture was not a factor (Idso et al, 1975b).

Since the surface temperature vs near-surface water content relationships established during controlled ground experiments were very promising (correlation coefficients exceeding 0.8 were obtained by Idso et al, 1975b), they were considered as a possible model for soil moisture monitoring from space. It was felt desirable to evaluate the effect of varying field and environmental conditions on the soil surface temperature — water content relationship. During 1976, the Canada Centre for Remote Sensing (CCRS), in co-operation with the Canada Department of Agriculture (CDA) and the Alberta Department of Agriculture, conducted an airborne experiment to determine how well the relationship holds over a larger agricultural area, what the effect of soil texture is on this relationship and how it can be removed, and if the estimation of soil moisture content could be improved by employing additional remote sensing data.

MATERIALS AND METHODS

The study was carried out along an east-west line 32 km long south of Lethbridge, Alberta; approximate co-ordinates of the site centre are 49°27' N, 112°42' W. The site is in an agricultural area and includes irrigated and non-irrigated land. Four airborne missions were undertaken (Table 1) composed of one flight in the early afternoon and another after midnight, except for Mission 2 which was delayed (day flight) and aborted (night flight). During each flight, thermal infra-red line scanner data (Cihlar and Brown, 1977) were obtained with a 1.7 milliradian (Mission 1, 2, 3) or 2.5 milliradian (Mission 4) sensor. In addition, multi-band or colour film photographic data were also acquired during daytime flights (Table 1). Multi-band photographs were processed as negatives and the colour film as a positive.

Twenty-four fields were selected along the flight line. During Mission 1 and Mission 4, nearly all fields were fallow. For Missions 2 and 3, twelve fields were fallow, one planted with flax and the remaining eleven were planted with barley. In each field, sites were located near the road for repeated sampling during each mission. Figures 1(a), (b) and (c) show a typical fallow field during three missions. Samples were collected from two sites within each field (Figure 2) for gravimetric soil moisture determination. At each site, samples were taken at four depths (0-2, 2-4, 4-10 and 10-20 cm) from two locations five metres apart; the number of sub-samples varied with depth. Sampling usually commenced at 10:30 Local Solar Time (LST) and 22:30 LST and lasted four hours. During the afternoon sampling, vertical and oblique ground photographs were taken and plant weight, percentage of straw cover at the surface, and surface roughness were also determined. Apparent temperature measurements were made for eight fields with a PRT-5 radiation thermometer held vertically at one metre above the surface. Within several days of Missions 2 and 4, undisturbed soil samples were taken from the 0-5cm and 10-15cm depths of each field and used to determine bulk density values for individual layers through interpolation. Undisturbed cores, 15cm long, were extracted from six fields representing the various soils along the test site. In addition, disturbed samples were taken from each field and analyzed for particle size distribution and salt content.

Soil moisture characteristic curves in the tension range 0 to 500cm, a 15 bar water content and bulk density were obtained for each undisturbed core. Correlation matrix between sand, silt, clay, and 0.33 bar percentage showed that the best predictor for the 0.33 bar water content for the soils involved (assumed to equal field capacity) was the amount of sand (0.2mm — 2.0mm). The amount of clay reduced the remaining unexplained variability insignificantly. Therefore, the following regression equation was computed:

$$\begin{aligned} FC &= 0.4022 - 0.00254S, \\ r^2 &= 0.725, n = 7, \text{ s.e.} = 0.022 \text{ g/cm}^3 \end{aligned} \quad (1)$$

where S is the amount of sand in percent for each field.

An inspection of calculated soil water contents indicated that, contrary to both theory and experimental results obtained during clear sky diurnal periods (Jackson et al, 1976), nighttime water contents were sometimes lower than those in the afternoon for the same sites. This discrepancy was probably caused by inaccurate depth measurements of the top layers at night, as moisture content increased with depth in all cases. For this reason, night moisture measurements

Table 1
Airborne Data Characteristics

Mission	Date (1976)	Time of Flight (U.S.T)	Air Temperature (°C)		Meteorological Data*		Relative Humidity (%)		Site Conditions Prior to and During Overflights			Data*** Collected
			Maximum	Minimum	Maximum	Minimum	Minimum	Maximum	Cloud Cover** (%)	Wind	Dew	
1	7 May	1340	21.2	4.5	82	29	29	5-10	Breeze	—	Package 1&2	
1	8 May	0110	25.7	7.6	76	22	22	0-5	None	—	Package 2	
2	1 June	1520	18.9	3.7	66	22	22	5-10	Moderate	—	Package 1&2	
3	5 July	1420	26.6	10.9	80	27	27	20-25	Gusty	—	Package 1&2	
3	6 July	0255	30.0	8.2	80	27	27	0-5	Low	Light	Package 1&2	
4	14 Sept	1340	25.4	5.7	77	20	20	0	None or	to Heavy	Package 3&4	
4		0030						0	Breeze	—	Package 4	

*Based on Leitchbridge Airport Weather Station data

**Of the total sky, estimated — Breeze < Low < Moderate

***Package 1: Kodak 2424 Pan IR film, 6" lens, 4 filters (Wratten 47B, 57A, 25, 88A)

Package 2: Thermal IR scanner imagery, 8-14 micrometres, resolution 1.7 milliradians

Package 3: Acrochrome Infra red film, 6" lens

Package 4: Thermal IR scanner imagery, 8-14 micrometres, resolution 2.5 milliradians

were used on moisture values. Frequently, the 0-4cm, 0-10cm were converted to 1

Proportions from in situ data which were used were employed. Table 2 gives measured for parent radian

$R_{0.2}$ (band

Similar site individual emul densitometer density variations of each site (frames) and t

For analysis converted to digital, digitized, and displayed on a monitor and known over each site for pixels with and nighttime site AT, was t

Mission	No.
1	1
2	2
3	3
4	4

*One flux field

**For each item.

Legend: PS —
PC —

PB — percent h

PH — plant he

were used only if they were higher than the corresponding afternoon values. To obtain site moisture values for each layer, the afternoon and night measurements were averaged; subsequently, the two locations within the site were averaged. Cumulative water contents for 0-2cm, 0-4cm, 0-10cm and 0-20cm were calculated by weighted averaging. These water contents were converted to PFC values using Equation (1).

Proportions of bare ground (PB), straw cover (PS), and plant canopy (PC) were compiled from in situ estimates, vertical ground photos, and oblique ground photos; both visual estimates which were repeatable to within about 10% and photographic density slicing (where possible) were employed to obtain the photo estimates. Plant heights (PH) were measured in the field. Table 2 gives ranges of these variables for Missions 1 to 4. Photographic densities (D) were measured for each site at each photo of the four bands (Missions 1, 2, 3) and converted to apparent radiances R_{app} using Equation (2):

$$R_{app}(\text{band}) = 10^D(\text{band}) \quad (2)$$

Similar site density measurements were made on colour film for Mission 4, except that individual emulsion layers were measured using the neutral, blue, green and red filters of a spot densitometer. Since the film was a positive, D was the exponent used in Equation (2). To reduce density variations due to both sun/surface cover geometry and vignetting, density measurements of each site were made on two to four photographs (possible because of overlap of adjacent frames) and the readings were averaged.

For analysis, airborne thermal scanner measurements recorded during the flights were converted to digital form (256 levels). Since the lower and upper scanner reference signals were also digitized, accurate apparent temperature values could be obtained. The digitized data were displayed on the CCRS MAD/MICA image processing system. Using software-controlled cursor and known distances from landmarks to sampled sites, a 5m x 10m rectangle was positioned over each site, and apparent temperature statistics (mean, standard deviation) were computed for pixels within the rectangle. The same procedure was repeated for all sites on both afternoon and nighttime imagery. The maximum-versus-minimum surface temperature difference for a site ΔT , was then obtained by subtracting the two means.

Table 2
Ranges of Ground Variables for Fallow Fields*

Mission	No. of Data Points	Ranges of**							
		PFC Values At Depths				PS	PB	PH	PC
		0-2	0-4	0-10	0-20	(%)	(%)	(cm)	(%)
1	48	32.2	48.5	61.9	75.3	3.0	30.0	0.0	0.0
		70.6	78.0	112.6	127.4	70.0	92.0	9.0	10.0
2	24	10.9	14.8	33.0	42.7	15.0	40.0	0.0	0.0
		54.6	56.2	64.5	84.9	60.0	85.0	15.0	15.0
3	24	10.6	26.9	55.2	69.7	10.0	25.0	0.0	0.0
		29.5	45.9	75.4	94.8	63.0	90.0	17.0	23.0
4	48	13.1	22.2	47.1	59.4	0.0	0.0	0.0	0.0
		67.9	74.6	110.6	122.3	82.0	100.0	56.0	100.0

*One flax field included for Missions 1 and 4.

**For each item, the maximum value is placed below the minimum value.

Legend: PS — percent straw
PC — percent plant cover

PB — percent bare surface
PH — plant height

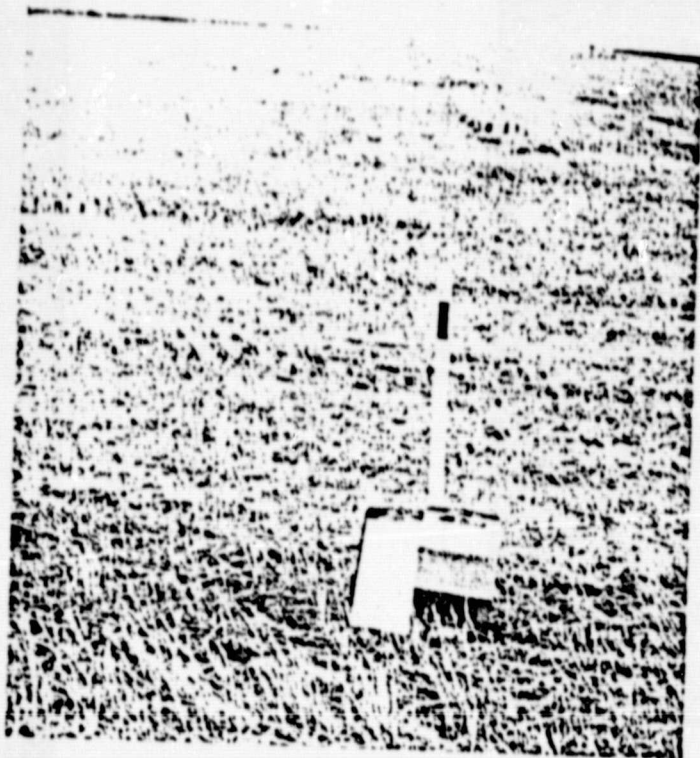


Figure 1 (a)
 Typical fallow field during
 Mission 1, May 1976



REPRODUCIBILITY OF THE
 ORIGINAL PAGE IS POOR



Figure 1 (b)
 Typical fallow field during Mission 3, July 1976

FIELD





Figure 1(c)
Typical fallow field during
Mission 4, September 1976

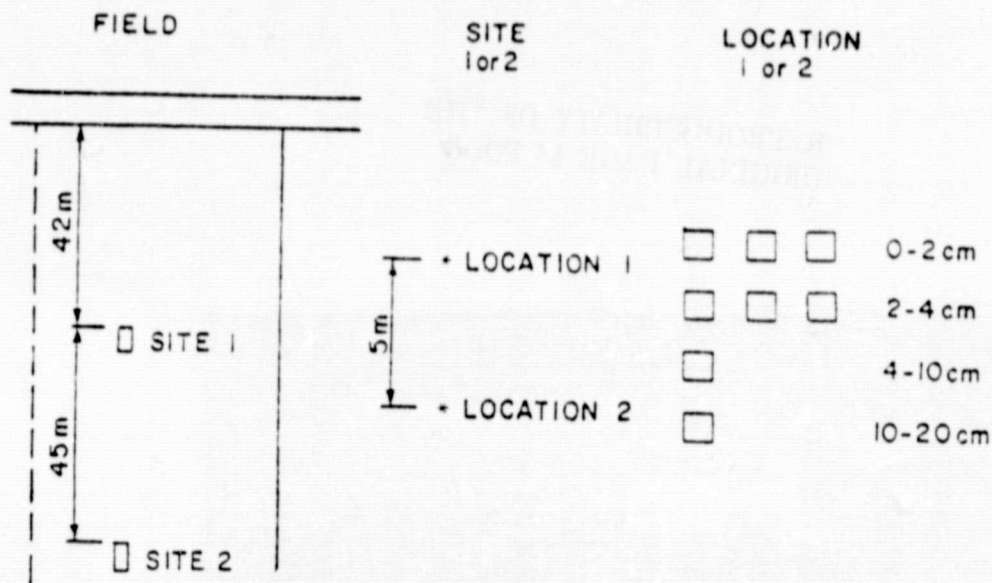


Figure 2
Sampling scheme for soil water content determination

RESULTS AND DISCUSSION

Data from each mission were analyzed separately because of the time delay of Mission 2 (Table 1) which apparently obliterated the temperature response to soil moisture, and problems with absolute calibration of one reference plate which occurred during Mission 1.

Effect of Soil Water Content

Figure 3 shows the relationship between the day minus night surface temperature differential (ΔT) and soil water content in the top 2cm expressed in percent of field capacity (PFC) for Mission 1. Although the inverse linear relationship was clearly defined, appreciable scatter of data points occurred along the ΔT axis. While the scatter was enhanced by points in the upper right and lower left positions representing only three fields, it would exist even if these fields were ignored. The differences between fields appeared real because site variability was relatively small; the within-site standard deviation of apparent temperature was typically less than 1°C . The scatter may be partly attributed to uncertainties in soil moisture determination, since the average within-site standard deviation of PFC values was 8% and the additional uncertainty introduced by Equation (1) was of similar magnitude.

The ΔT vs PFC (0-2cm) plot for Mission 3 is shown in Figure 4. All fallow fields were dry as evidenced by the narrow range of PFC values. However, the spread of temperature differentials was larger than for the other missions. Mission 4 data (Figure 5) exhibited a well defined inverse linear relationship between ΔT and PFC (0-2cm). The scatter in the ΔT direction was of similar magnitude as for Mission 1, i.e. the scatter was larger at lower PFC values (the two data points near $\Delta T = 15^\circ\text{C}$ represent a flax field). Compared to Mission 3, Mission 4 values were lower by a constant offset (6°C) as both calculated linear regression lines had a slope of $-0.13^\circ\text{C}/1\%$ PFC.

Correlation coefficients r between PFC and ΔT , for individual missions are shown in Figure 6 and with the exception of Mission 3, r values were highest for the top layer (0-2cm) and decreased with depth. The low Mission 3 value was probably due to the narrow PFC range, as correlation coefficients for deeper layers were similar to those from other missions. Secondly, r values for the 0-4cm layer were consistent throughout the season and almost as high as for the 0-2cm layer. Correlation coefficients for both layers improved when Mission 3 and Mission 4 data were combined, possibly due to a wider range of PFC values and a higher slope of the combined data set. Correlation between ΔT and PFC of deeper layers was generally low and inconsistent, thus suggesting a poor response of surface temperatures to water contents in deeper layers.

Effect of Surface Cover on ΔT

Figure 7 shows absolute values of correlation coefficients between ΔT and ground variables measured for fallow fields. Single and multiple correlation coefficients are given for individual and combined (3 + 4) missions and two layers, 0-2cm and 0-4cm. With the exception of Mission 4, near-surface soil water content was the most important variable. Mission 4 was flown shortly after harvest, and large portions of fields were covered with a mulch of fresh straw (40% of all fields had straw cover of 60% or higher); this factor was probably responsible for the high correlation. Compared to Figure 7, correlation coefficients for PB, PH, PC and PS would change to 0.81, -0.19, -0.32 and -0.80 respectively if the flax field data were omitted from Mission 4. For Missions 1 and 3, the straw mulch did not have a significant effect on measured ΔT values.

Multiple linear regression calculations indicate (Figure 7) that the surface parameters tested accounted for approximately 30% to 85% of total ΔT variability depending upon data set; Mission 3 surface layer was the lowest with only 8% of ΔT explained.

Only marginal improvements of multiple correlation coefficients were obtained after including surface cover descriptors (Figure 7). Mission 4 was the exception to this trend, as the proportion of bare ground (closely related to PS) increased the correlation coefficient substantially.

The effect of surface roughness was detected only with the PRT-5. A series of measurements made in September 1976 showed a definite inverse relationship between the

surface-air temperature differential and soil moisture (top 2cm). The lines for individual fields had an identical slope but were displaced vertically over a 4°C range. A comparison of surface roughness estimates for individual measurements indicated that smooth surfaces exhibited higher temperatures for equivalent water contents than rough surfaces. It appears that this effect was related to the sunlight/shadow ratio as determined by the solar zenith angle. The effect was not evident in the airborne data, probably because all fallow fields appeared equally rough for the selected cursor size.

The consistently high ΔT_s sensitivity to near-surface soil water content is encouraging, particularly since it persisted under natural conditions encompassing various soil, surface, roughness, straw cover and to some extent green vegetation conditions. Reasons for the low multiple correlation coefficients are not clear. Atmospheric or sensor effects may be excluded because the flight line was relatively short and the analysis was carried out for each mission separately. One reason might be inaccurate ground cover data. It should be noted, however, that apparent temperatures did not change substantially outside of the 5m x 10m rectangles delineated at each site as determined by enlarging the rectangle to 5m x 30m. Although the standard deviation increased somewhat, the mean value seldom varied by more than 1°C. This suggests that the surface conditions over a larger area were similar to those at the sampled sites, and thus the single set of ground cover estimates per field should be adequate. Another possible reason for the low multiple correlation coefficients shown in Figure 7 is the uncertainty of soil moisture estimates discussed previously. If this explanation is valid, it will imply better ΔT_s vs PFC correlation than indicated in Figures 3, 4 and 5.

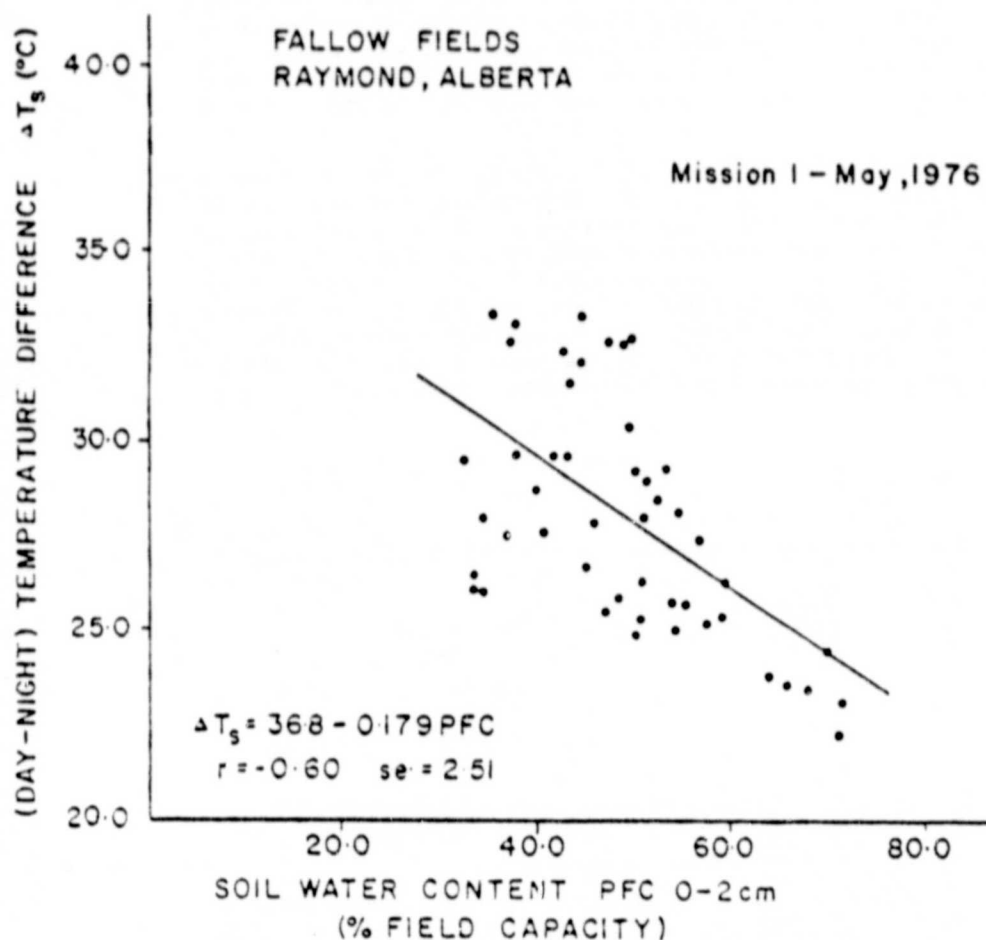


Figure 3
Diurnal soil surface temperature differential: ΔT_s , as a function of water content in top 2cm of fallow fields:
Mission 1, May 1976

Effect of Soil Texture on ΔT_s

Correlation coefficients between ΔT_s and two measures of soil water content, percent of field capacity and volumetric water content are given in Table 3. Soil texture was clay loam (8 fields), clay (8), loam (4), and sandy clay loam (4). A decrease of r values for all cases is evident. The "difference" column in Table 3 indicates that an additional 5 to 26% of the total variability in the ΔT_s vs soil water content relationship could be explained when PFC was used as the soil water parameter.

Table 3 suggests that about an additional 15% of the total variability could be accounted for with PFC as the soil water content parameter. Considering that this fraction would increase further for a wider range of soil textures, it appears that the use of a tension-related measure of soil water for the thermal emission method is unavoidable. This is not necessarily a disadvantage since tension is a better indicator of soil water behaviour than water content; however, the use of a ΔT_s vs tension relationship would require the development of accurate predictive models.

Stability of the ΔT_s vs PFC Relationship

A single, time-invariant soil water vs ΔT_s relationship would ideally be required for determining soil moisture remotely from thermal emission measurements. Since air temperature has a significant effect upon surface temperatures, temporal variations of air temperatures increase the uncertainty of soil water prediction. A procedure for removing air temperature effects from measured ΔT_s values was developed by Idso et al (1976) and used by Millard et al (1978).

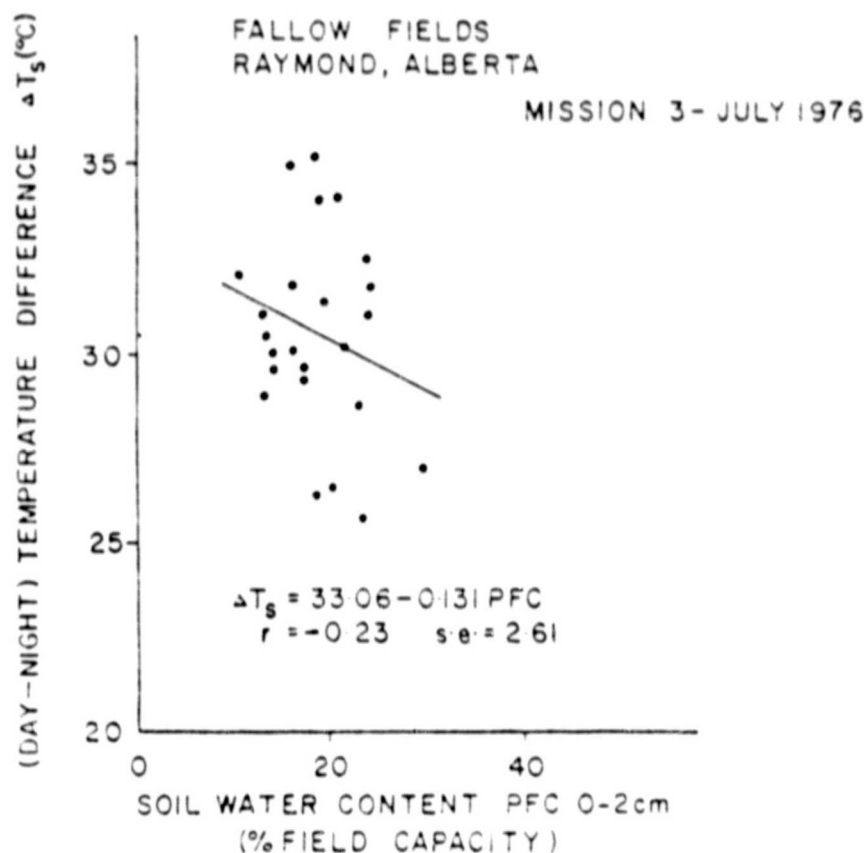


Figure 4

Diurnal soil surface temperature differential ΔT_s , as a function of water content in top 2cm of fallow fields: Mission 3, July 1976

Table 3

Effect of Soil Texture On ΔT_s vs Soil Water Content Relationship

Mission	Depth (cm)	Correlation (ΔT_s , PFC)	Coefficient r (ΔT_s , m.)	Difference in r^2 (%)
1	0-2	-0.60	-0.45	16
	0-4	-0.53	-0.17	25
3	0-2	-0.23	-0.07	5
	0-4	-0.57	-0.26	26
4	0-2	-0.68	-0.62	8
	0-4	-0.64	-0.52	14
3 + 4	0-2	-0.77	-0.72	7
	0-4	-0.72	-0.62	13

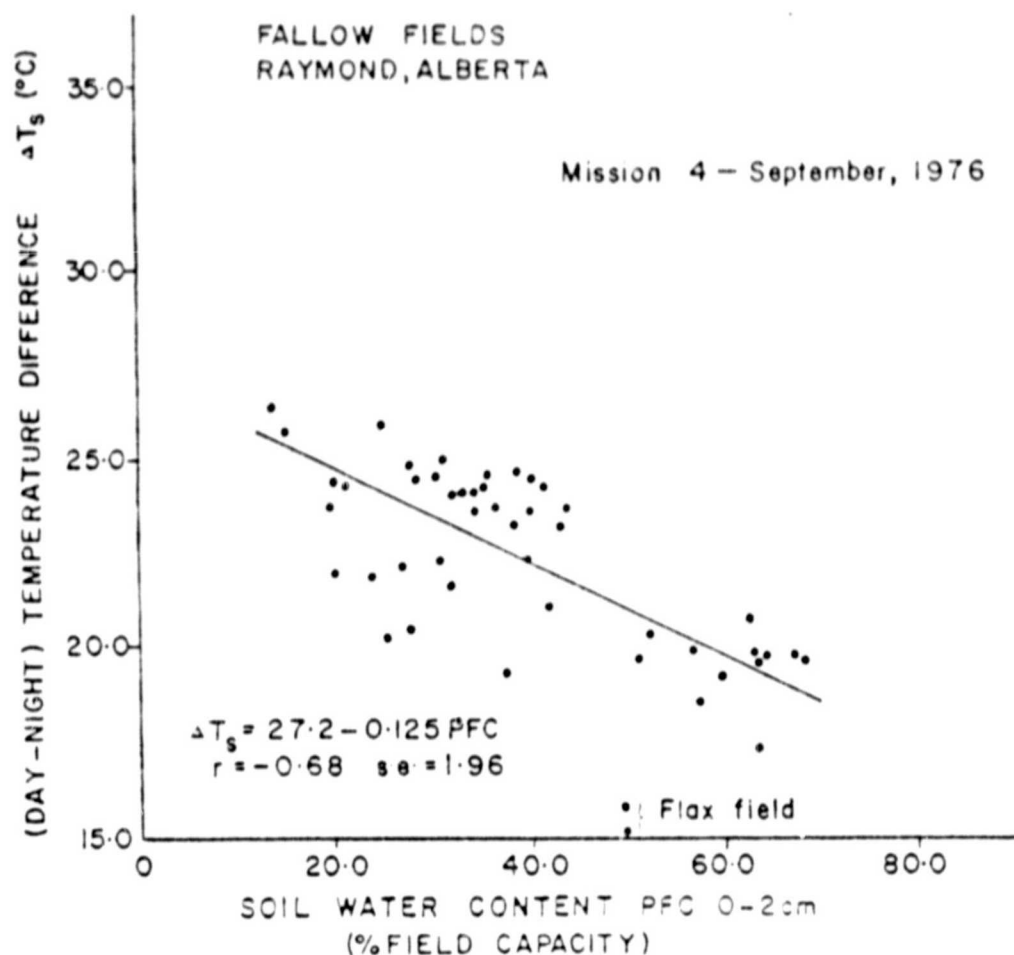


Figure 5

Diurnal soil surface temperature differential ΔT_s , as a function of water content in top 2cm of fallow fields: Mission 4, September 1976

Table 4

Diurnal Air Temperature Differentials ΔT_a and Regression Parameters for Three Missions

Mission	ΔT_a (°C)	Regression* Between ΔT_a and PFC (0-2cm)	
		Intercept (°C)	Slope (°C/1% pFC)
1	15.0	36.8	-0.179
3	17.0	33.6	-0.131
4	21.0	27.22	-0.125

*Equation has the form:

$$\Delta T_a = \text{Intercept} + (\text{Slope})(\text{PFC } (0-2))$$

It involves calculation of normalized ΔT_{an} as follows:

$$\Delta T_{an} = \frac{\Delta T_a}{\Delta T_{an}} \Delta T_{an}$$

where ΔT_a is the difference between maximum and minimum air temperatures for the diurnal period of interest, and ΔT_{an} is the normalizing air temperature differential chosen as 18°C in references quoted above. When applied to data herein, the normalization should result in merging the three regression lines into one.

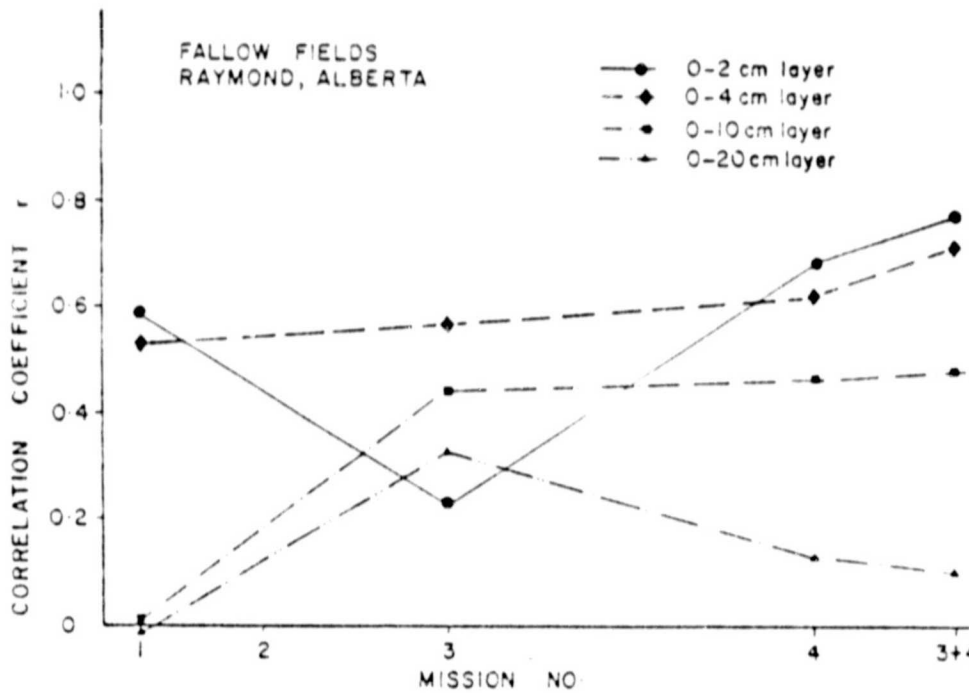


Figure 6

Correlation coefficient between the diurnal soil surface temperature differential ΔT_a and water content for four soil layers for various missions: fallow fields

Table 4 gives slopes and intercepts of the ΔT , vs PFC (0-2cm) relationships and ΔT , obtained as averages from surrounding meteorological stations for Missions 1, 3 and 4. Since Equation (3) should hold for all PFC values including 0%, the ratio of intercept to ΔT , should be constant for the three missions. However, this ratio varied between 1.3 (Mission 4) and 2.5 (Mission 1) for data in Table 4. Consequently, use of this equation would increase rather than reduce the differences among individual missions

Assuming Equation (3) to be sound, discrepancies among individual data sets must be related to environmental conditions affecting the measurements or to the thermal scanners used. The high slope and intercept values for Mission 1 probably were due to faulty absolute calibration of the high temperature range which was detected during post-mission tests. Although within-mission comparisons remain valid, comparing results to other missions would not be warranted. On the other hand, scanners for Missions 3 and 4 were calibrated and the discrepancy between the data sets must be related to environmental conditions. Graphic and statistical analyses consistently showed that straw mulch cover was not responsible for the lower intercept of Mission 4. The atmosphere was somewhat hazy prior to the afternoon flight which could reduce the solar energy input and consequently lower surface temperatures somewhat. Also, the

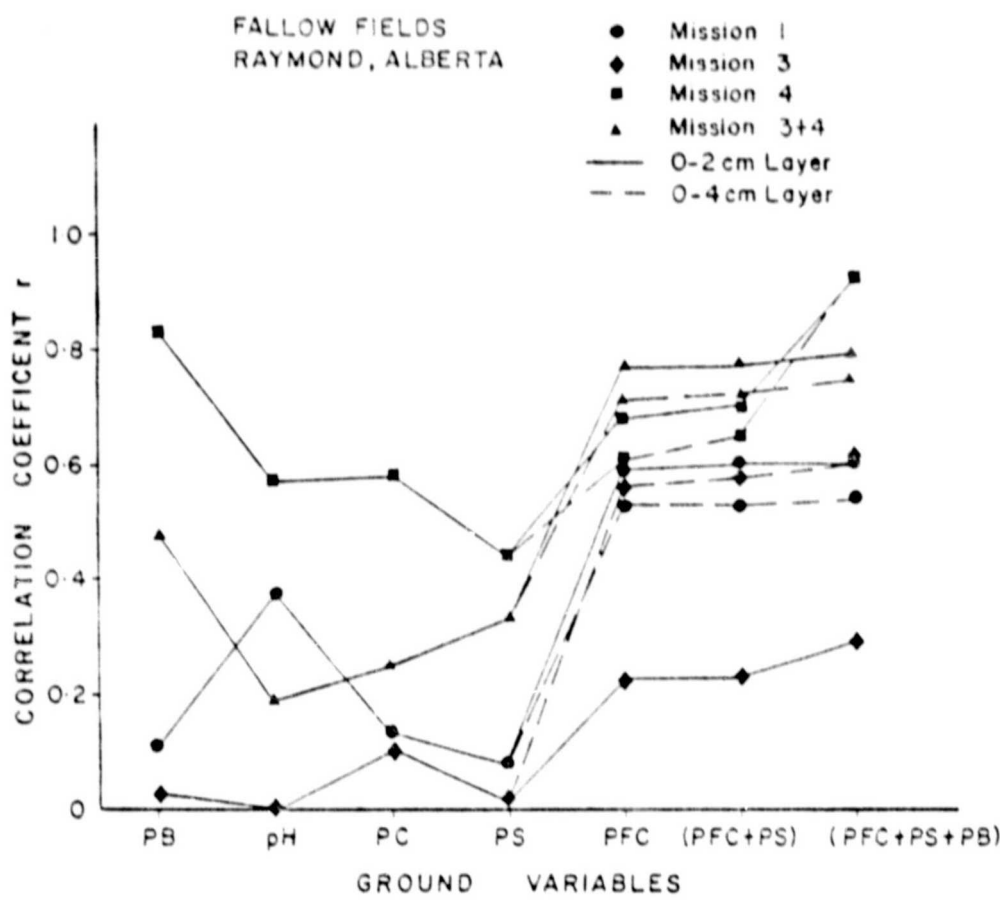


Figure 7

Single and multiple correlation coefficient values between the diurnal soil surface temperature differential ΔT , and various ground variables: PB = percent bare ground, PH = plant height (cm), PC = percent plant cover, PS = percent straw cover, PFC = percent field capacity

wind was higher prior to and during Mission 4 (25km/h) than for Mission 3 (18km/h). Nevertheless, these factors do not appear to explain sufficiently the 7°C difference in intercepts. In fact, the Mission 4 intercept should be about 25% higher for the ΔT_s values given in Table 4 in order for Equation (3) to eliminate differences between the missions. Since diurnal air temperature extremes were consistent for all surrounding meteorological stations, they do not appear to be the cause of the discrepancy.

One reason for the observed lower intercept value for Mission 4 may be solar radiation. The solar noon zenith angle was 26.6° for Mission 3 and 45.7° for Mission 4. Since solar radiation incident on a horizontal surface is directly proportional to the cosine of the zenith angle, about 25% more radiation would be received during Mission 3. It is worth noting that the Mission 3 intercept was 21% higher than that for Mission 4. The zenith angle explanation does not account for increasing the discrepancy between intercepts by applying Equation (3), however.

Effect of Reflected Solar Radiation

Figure 8 shows absolute values of single and multiple correlation coefficients between PFC (0-2cm) and remote sensing measurements. B1 through B4 represent apparent radiances for bands 1 through 4 (approximate wavelength ranges: B1 = 0.38 to 0.47 micrometres; B2 = 0.47 to 0.59 micrometres; B3 = 0.59 to 0.71 micrometres; B4 = 0.71 to 0.95 micrometres) determined as described under Materials and Methods. Correlation between PFC (0-2cm) and apparent spectral radiances was statistically significant for Missions 3 and 4 ($P < 0.01$), but was not consistent as evident from Mission 1 data. Since the surface soil of practically all fields was dry during the missions, the correlations for Missions 3 and 4 should be due to the relationship between surface cover and near-surface soil moisture. This was confirmed by multiple correlation analysis between PFC (0-2cm) and surface cover parameters which resulted in r values around 0.6 for Missions 3 and 4.

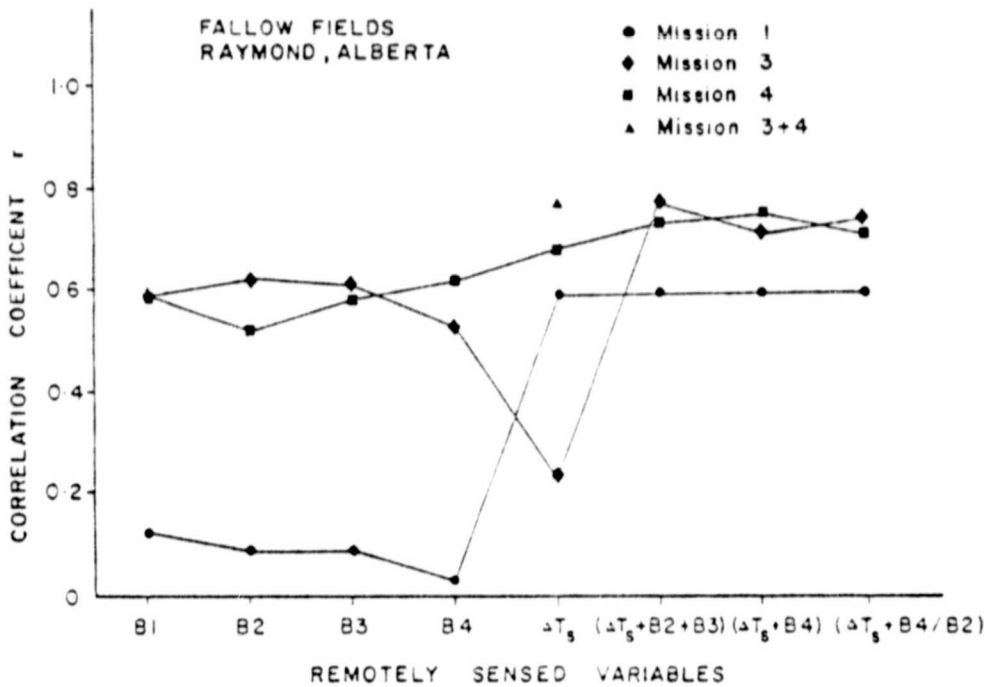


Figure 8

Single and multiple correlation coefficients between soil water content in top 2cm and several remotely sensed variables: B1 to B4 = apparent reflectance in four bands (0.38 to 0.47 micrometres, 0.47 to 0.59 micrometres, 0.59 to 0.71 micrometres, 0.71 to 0.95 micrometres); ΔT_s = diurnal soil surface temperature differential

REPRODUCIBILITY OF THE ORIGINAL PAGE IS POOR

Results shown in Figure 8 indicate that the addition of radiance data improved the accuracy of soil moisture estimation. The degree of improvement varied from high (Mission 3) to negligible (Mission 1). Due to film differences between Missions 3 and 4, their apparent radiances could not be combined. Since the soil water content range for Mission 3 was rather narrow, Missions 1 and 4 are probably more characteristic of the improvements in predictive accuracy that may result from including visible bands data. It is encouraging that the r values for the combination involving the band ratio were almost as high as for the actual values because ratios do not require data with absolute calibration. Considering the relatively crude measurement technique used to obtain the apparent radiance data, the results shown in Figure 8 should be treated with care. Evidently, some improvement of the predictive accuracy is possible, and a detailed study of this problem should be undertaken.

SUMMARY AND CONCLUSIONS

A study of the relationship between diurnal surface temperature variations and near-surface soil water content yielded the following results:

- 1) Under clear sky condition, an inverse linear relationship existed between the day minus night surface temperature differential (ΔT_s) and soil water content expressed in percent of field capacity (PFC) in the top 2 to 4cm of soil.
- 2) With the exception of the post-harvest Mission 4, near-surface water content was the most important ground variable, even under considerable straw mulch cover.
- 3) The variability of ΔT_s vs soil water relationship was reduced appreciably when soil texture was taken into account.
- 4) The temporal stability of the PFC vs ΔT_s relationship did not improve when diurnal air temperature variations were taken into account.
- 5) The relationship between PFC and ΔT_s improved to various degrees when apparent radiances from the visible spectrum were also included; correlation coefficients approached 0.8 (0.7) for the top 2cm (4cm) of the soil, respectively.

Results of this study indicate that the diurnal surface temperature variations correspond fairly closely to near-surface water content in fallow fields with various straw mulch, roughness, soil texture and seasonal conditions. Effects of other variables (surface slope, variable cloud cover) have not yet been examined. Future studies should include such variables, attempt to maximize the accuracy of soil water content prediction by using additional remote measurements, and development of a time-invariant, generally applicable predictive algorithm. If these problems are successfully solved, the thermal emission technique should become a useful tool for routine soil moisture surveys of fallow fields.

REFERENCES

- Cihlar, J. and Ulaby, F.T. 1975 — *Microwave Remote Sensing of Soil Water in Agricultural Fields*, Technical Report 264-5, Remote Sensing Laboratory, The University of Kansas Center for Research Inc., Lawrence, Kansas.
- Cihlar, J. 1976 — *Soil Moisture Determination by Thermal Infra-red Remote Sensing*, Proceedings of the Workshop on Remote Sensing of Soil Moisture and Ground Water, 8-10 November 1976, Toronto, Ontario, pp.206-215.
- Cihlar, J., and Brown, R.J. 1977 — *Aerial Heat Loss Detection from Buildings*, Engineering Digest 23(10), pp.29-31.

- Idso, S.B., Jackson, R.D. and Reginato, R.J. 1976 — *Compensating for Environmental Variability in the Thermal Inertia Approach to Remote Sensing of Soil Moisture*, *Journal of Applied Meteorology* 15, pp.811-817.
- Idso, S.B. and Ehler, W.L. 1976 — *Estimating Soil Moisture in the Root Zone of a Plant: A Technique Adaptable to Remote Sensing*, *Geophysical Research Letters* 3, pp.23-25.
- Idso, S.B., Jackson, R.D. and Reginato, R.J. 1975(a) — *Detection of Soil Moisture from Satellite Surveillance*, *American Scientist* 63, pp.549-556.
- Idso, S.B., Schmugge, T.J., Jackson, R.D. and Reginato, R.J. 1975(b) — *The Utility of Surface Temperature Measurements for the Remote Sensing of Soil Water Status*, *Journal of Geophysical Research* 80, pp.3044-3049.
- Jackson, R.D., Reginato, R.J. and Idso, S.B. 1976 — *Timing of Ground Truth Measurements During Remote Assessment of Soil Water Content*, *Remote Sensing of Environment* 7, pp.247-255.
- Millard, J.P., Jackson, R.D., Goettelman, R.C., Reginato, R.J. and Idso, S.B. 1976 — *Water-Stress Assessment Using an Airborne Thermal Scanner*, *Photogrammetric Engineering and Remote Sensing* 44, pp.77-85.
- Reginato, R.J., Idso, S.B., Vedder, J.F., Jackson, R.D., Blanchard, M.B. and Goettelman, R.C. 1976 — *Soil Water Content and Evaporation Determination by Thermal Parameters from Ground-based and Remote Measurements*, *Journal of the Geophysical Research* 81, pp.1617-1620.
- Schmugge, T., Blanchard, B., Anderson, A. and Wang, J. 1978 — *Soil Moisture Determination from Aircraft Observations of the Diurnal Range of Surface Temperature*, *Water Resources Research* 14, pp.169-172.

The following proceedings are available from the Canadian Aeronautics and Space Institute:

1. **First Canadian Symposium on Remote Sensing**
February 1972, Ottawa. 764 pp. Price \$10.00 Can.
2. **Second Canadian Symposium on Remote Sensing**
29th May - 1st June 1974, Guelph. 739 pp. 2 Vols. Price \$52.00 Can., \$53.00 outside Can.
3. **Third Canadian Symposium on Remote Sensing**
22nd - 24th September 1975, Edmonton. 516 pp. Price \$41.00 Can., \$42.00 outside Can.
4. **Fourth Canadian Symposium on Remote Sensing**
15th - 18th May 1977, Quebec City. 613 pp. Price \$41.00 Can., \$42.00 outside Can.
5. **Remote Sensing of Soil Moisture and Groundwater**
8th - 10th November 1976, Toronto. 242 pp. Price \$26.00 Can., \$27.00 outside Can.
6. **Fifth Canadian Symposium on Remote Sensing**
28th - 31st August 1978, Victoria. 602 pp. Price \$41.00 Can., \$42.00 outside Can.

REPRODUCIBILITY OF THE
ORIGINAL PAGE IS POOR